

2023

Evolution of residual solid stresses and viscoelastic properties in murine brains by age

<https://hdl.handle.net/2144/45455>

"Downloaded from OpenBU. Boston University's institutional repository."

BOSTON UNIVERSITY
COLLEGE OF ENGINEERING

Thesis

**EVOLUTION OF RESIDUAL SOLID STRESSES AND
VISCOELASTIC PROPERTIES IN MURINE BRAINS BY AGE**

by

SIYI ZHENG

B.S., Hunan University, 2021

Submitted in partial fulfillment of the
requirements for the degree of
Master of Science

2023

© 2023 by
SIYI ZHENG
All rights reserved

Approved by

First Reader

Hadi T. Nia, Ph.D.
Assistant Professor of Biomedical Engineering
Assistant Professor of Materials Science and Engineering

Second Reader

Béla Suki, Ph.D.
Professor of Biomedical Engineering
Professor of Materials Science and Engineering

Third Reader

Paul E. Barbone, Ph.D.
Professor of Mechanical Engineering
Professor of Materials Science and Engineering

**EVOLUTION OF RESIDUAL SOLID STRESSES AND
VISCOELASTIC PROPERTIES IN MURINE BRAINS BY AGE**

SIYI ZHENG

ABSTRACT

Residual solid stresses are mechanical forces generated and transmitted by solid components of tissue. Here, we quantified the residual solid stress developed in the brain and kidney by tissue slicing. By this method, we showed that murine brains contain higher residual solid stresses than murine kidneys, which were previously shown to have negligible residual solid stress. Since development and aging differentially affects residual solid stress in each organ, we utilize the slicing method to quantify the evolution of residual solid stresses in brains from mice which are 5–7 days old to 22 months old. We found that residual solid stresses increase rapidly in the early stages of tissue growth and development. We also evaluated the changes of viscoelastic properties in the murine brain with age to analyze the relationship between viscoelastic properties and residual solid stress changes, and their potential connection with tissue development. Additionally, we tested the whole brain from adult mice with a slicing method to evaluate the distribution of residual solid stress.

TABLE OF CONTENTS

ABSTRACT.....	iv
LIST OF FIGURES.....	vii
INTRODUCTION.....	1
MATERIALS AND METHODS.....	4
Mice Strain.....	4
Slicing method.....	4
Releasing residual solid stress.....	4
Tissue imaging and post-processing.....	5
Measurement of viscoelastic properties.....	6
Unconfined compression test.....	6
RESEARCH AIMS AND DESIGN.....	9
Aim 1: Optimize and validate residual solid stress quantification methodology in the murine organs.....	9
Quantify residual solid stress with normalized deformation as an index of residual solid stress.....	9
Micron-scale of deformation map.....	11
Ionic strength effect to deformation.....	11
Validation experiments.....	12
Aim 2: Map evolution of residual solid stress changes in the murine brain with age..	13
Evolution of residual solid stress in murine brain with age.....	13
Evolution of viscoelastic properties in murine brain with age.....	13

Residual solid stress distribution in the whole brain	14
RESULTS.....	15
Aim 1	15
Quantify residual solid stress with normalized deformation as an index of residual solid stress	15
Micron-scale of deformation map	16
Ionic strength effect to deformation	16
Validation experiments	18
Aim 2	21
Evolution of residual solid stress in murine brain with age	21
Evolution of viscoelastic properties with age	22
Residual solid stress distribution in whole brain	23
DISCUSSION.....	25
CONCLUSION.....	27
BIBLIOGRAPHY.....	28
CURRICULUM VITAE.....	30

LIST OF FIGURES

Figure 1	6
Figure 2	8
Figure 3	8
Figure 4	10
Figure 5	15
Figure 6	16
Figure 7	17
Figure 8	18
Figure 9	19
Figure 10	20
Figure 11	22
Figure 12	23
Figure 13	24

INTRODUCTION

Residual solid stress is a kind of mechanical force which is generated and transmitted by solid components of tissue, and is closely related to organ growth and pathological change, and varies between different organs [1]. Stiffness is a traditionally studied biomechanical property, describes the extent to which a material resists deformation in response to an applied force. Residual solid stress, related to stiffness, is defined as force per area, and can cause either compression or tension of a material [2, 3]. Organs exert forces on surrounding tissue through mechanisms such as tissue growth and disease [4, 5] and cause tissue deformation and subsequent mechanical stress. As a result of these forces, the surrounding tissue returns an equal and opposite stress, termed externally-applied residual solid stress [3].

In abnormal tissues, mainly tumors, mechanical forces caused by rapid growth will compress the blood vessels and cells in the surrounding normal tissue. The collapse of vessels can adversely impact the health of tumor-bearing organs. The brain, which is unique from other extracranial organs because of the physical confinement by the skull, is greatly affected by mechanical compression forces that can cause devastating effects such as nerve damage [6]. As a result, the initial presentation of neurological symptoms, like impacted physiological function, are mostly the basis to diagnose a primary or metastatic tumor [7] in the brain. It is important to explore the origins and consequences of residual solid stress mechanistically.

In normal tissues, the stress field can tightly regulate tissue growth, remodeling and morphogenesis, and these processes can also conversely generate stress [8]. For

example, in arteries, changes in the systemic pressure can trigger growth [9]. In turn, as demonstrated by cell-generated traction forces during cytokinesis and the existence of residual stresses in various soft tissues, stress can be induced by growth and remodeling [10].

Development and aging are important factors contributing to residual solid stresses in tissues. As the body grows and develops, organs experience several structural changes. It is known that in humans, the brain goes through a prolonged and complex maturation process from embryo to the third decade, and progressive senescence from approximately the sixth decade [11, 12]. Previous research investigating growth charts for typical and atypical human brain development and aging demonstrated milestones and critical periods in brain maturation [13]. The brain grows most rapidly in the early stages of development, especially in the embryo stage [14], and reaches approximately 80% of its maximum size in the very early stages of life, the fastest development appearing in the first 3 years in humans' 100-year lifespan [15]. Due to rapid growth, there is an accumulation of residual solid stress inside the brain that affects its growth, development and ability to maintain its biological structure. Similarly, residual solid stress changes in the aged brain due to tissue atrophy, which can affect and indicate the appearance of progressive neurodegenerative disorders like Alzheimer [15]. Besides aging, pregnancy has been found to have a significant impact on the maternal brain which leading to changes in structure due to biological adaptations [16]. Such changes, especially the reductions in gray matter volume in regions subserving social cognition, could stay for at least 2 years post-pregnancy [17]. Thus, the study of residual solid stress at different ages

will be helpful to understand the development or disease of the brain, and also have the potential to help study the stress changes with structure in other biological conditions. Previous research has shown the existence of residual solid stress in the brain [18], but lacks quantification, and thus is not able to make comparisons of the residual solid stress level, and neither connect the stress changes with organ structure.

The brain is a soft organ which is protected by the skull and can be easily affected or damaged by application of mechanical forces to it. In brain tumors or neural diseases like Alzheimer's, the brain structure changes with compression or shrinking, which results in changes in residual solid stress [13, 19]. Thus, it is important to evaluate how the brain structure will vary with rapid growth in the early developmental stages of life and its potential decrease in volume with aging. Residual solid stress can indicate how the brain is developing and growing, and can also predict decline in function. Furthermore, it is important to study age-associated residual solid stress changes in the brain, which is known to shrink with aging, especially with neural diseases like Alzheimer's [15].

MATERIALS AND METHODS

Mice Strain

Mice were housed and bred under pathogen-free conditions at the Boston University Animal Science Center. All experiments conformed to ethical principles and guidelines under protocols approved by the Boston University Institutional Animal Care and Use Committee. All mice were C57BL/6 strains from three different age groups: 5–7 days, 8–12 weeks, and 22 months.

A breeding pair of transgenic mice, B6.129(Cg)-Gt(ROSA)26Sortm4(ACTB-tdTomato,-EGFP)Luo/J (JAX #007676, Jackson lab, ME) hereafter referred to as mTmG, was purchased to start a colony and was the primary source of all animals for the experiments. Mice from 5–7 days and 8–12 weeks had mTmG fluorescence reporter. Mice from 22 months were wild type (provided from Connizzo lab) and the slices were stained with DAPI to visualize the nuclei. N=4, 6, 8 mice were used for age groups 5–7 days, 8–12 weeks, and 22 months, respectively.

Slicing method

Releasing residual solid stress

2% agarose is prepared using low gelation temperature agarose (Sigma-Aldrich) mixed with phosphate-buffered saline (PBS). The 2% agarose solution is in a liquid state at a temperature of 40 °C. The organs, including brain and kidney, were immediately extracted post-euthanasia through CO₂, and embedded in 2% agarose in a stainless-steel cast provided by the commercial vibrating microtome, Compresstome (F00395A, Precisionary Instruments LLC). The agarose-embedded organs are fully immersed in

PBS and sliced via the Compressstome to the desired thickness of 250 μm which is thin enough for showing the deformation, but thick enough to avoid the tissue being broken by handling (Fig. 1A). The tissue slice is detached from the agarose slice spontaneously or manually with a pair of sharp tweezers, collected in a 24-well plate, and immersed in PBS for 20 minutes at room temperature to allow the tissue to release any residual solid stresses in the tissue (Fig. 1B). As a result of stress relaxation, the tissue slice becomes deformed. Then the PBS is removed and the slice is embedded in 1% agarose to hold the deformation. The tissue slice is fixed for 4 hours in 10% formalin to avoid the tissue degradation and then washed and stored in PBS refrigerated (Fig. 1C). Mice from 22 months were wild type and the tissue slices were stain with DAPI (Thermo Fisher), which is a nuclear and chromosome counterstain and can emit blue fluorescence.

Tissue imaging and post-processing

With the fluorescence reporter in the tissue, the sample is imaged via Olympus FV3000 laser scanning confocal microscope using UPL SAPO10X2 (Olympus, NA 0.4, 10x magnification) air immersion objective lens (Olympus) at scanning resolutions between 512x512 pixels in FV31S-SW Viewer software (Olympus). Slices from 5–7 days and 8–12 weeks groups mice had tdTomato fluorescence and were imaged using a 561 nm excitation laser and 570–620 detection wavelength, the slices from 22 months group mice had DAPI fluorescence and were imaged using a 405 nm excitation laser and 430–470 nm detection wavelength. The tissue-agarose construct that is immersed in PBS was imaged to get the 3D structure (Fig. 1D). The 3D images are exported from ImageJ to MATLAB for post-processing. The post-processing includes normalized deformation

calculation, and the reconstruction of the deformation map. The release of residual solid stress via slicing results in surface bending of the slice. The overall bending extent after slicing represents the area strain, a quantitative index for residual solid stress in the slice. We defined the normalized deformation as the average height difference from the curved surface to the midline. The deformation map shows the contribution of deformation in individual slices.

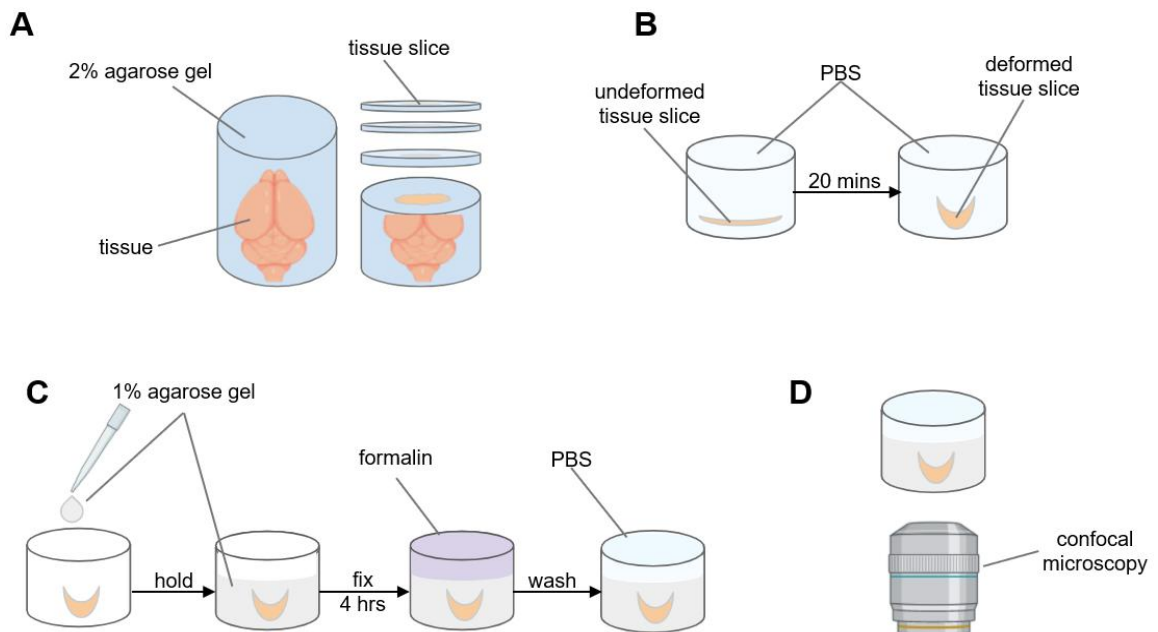


Figure 1 Methodology of deformation quantification. (A) The fresh tissue is embedded in 2% agarose, then sliced with a Compressstome for getting specific thickness. (B) Leave the slices in PBS at room temperature for 20 mins until the stress-induced deformation occurs. (C) The deformed slices are held in 1% agarose, then fixed with formalin and washed with PBS. (D) The deformed slice is imaged via confocal microscopy.

Measurement of viscoelastic properties

Unconfined compression test

The bulk viscoelastic properties of the tissues were measured via the instron 5900 Series System (Illinois Tool Works Inc) in macroscale with an unconfined compression test. Organs were sliced with the Compressstome using the slicing method with a 2mm

thickness. The slices were then punched with biopsy punches for 6mm diameter, and maintained in PBS with protease inhibitors at 4°C before mechanical testing. All measurements were performed in near-physiological PBS at room temperature. The sample was placed in a loading machine and set the point where the upper plate is in contact with the sample as 0 displacement (Fig. 2A), then applying a constant strain. Each specimen was compressed by 5% of original height in ramps of 1s and allowed to relax for 3 minutes. Four consecutive steps were performed to apply the displacement changing with time (Fig.2B). The instron then measured the force changes in the whole process, including the increase of force while compressing, and also the force decreasing during the relaxation time, and reached an equilibrium point (Fig.2C).

The plots of displacement versus time and force versus time were converted to plots of stress versus time and strain versus time. Stress was the ratio of force to surface area, and strain was the ratio of displacement to total thickness. The stress is then plotted as a function of strain, and the Young's modulus is estimated as the slope of the linear fit to the stress-strain data as modulus measurement (Fig. 3A). Instantaneous / equilibrium force ratio is the ratio of maximum force to equilibrium force, which indicates how much stress the tissue releases to reach an equilibrium point (Fig. 3B). The relaxation time constant was used to compare the time of how long it takes for the tissue stress level to relax (Fig. 3C).

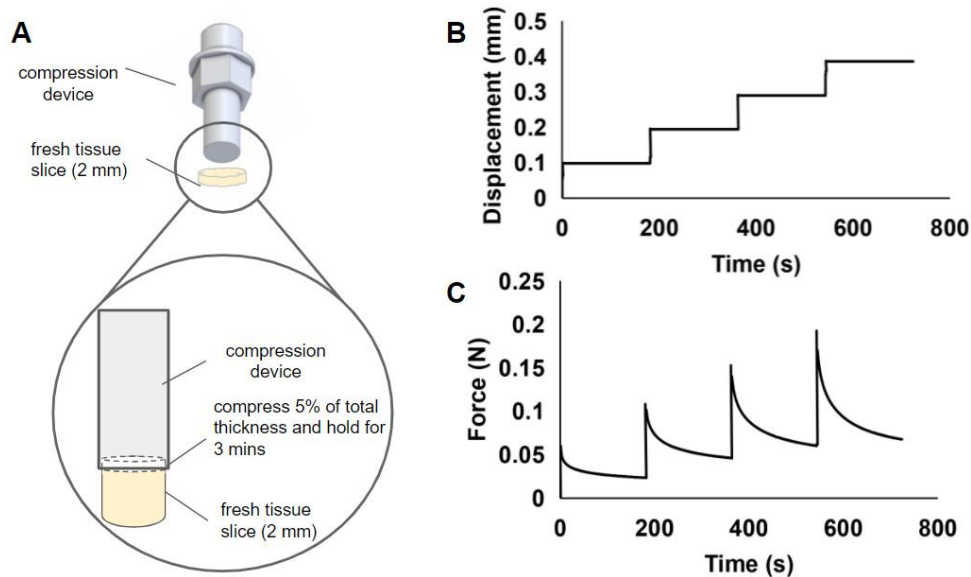


Figure 2 Methodology of viscoelastic properties quantification. (A) Unconfined compression test through instron. (B) Applied 4 consecutive steps of compressing with each step compress 5% of total thickness. (C) Measured force changes in the whole process.

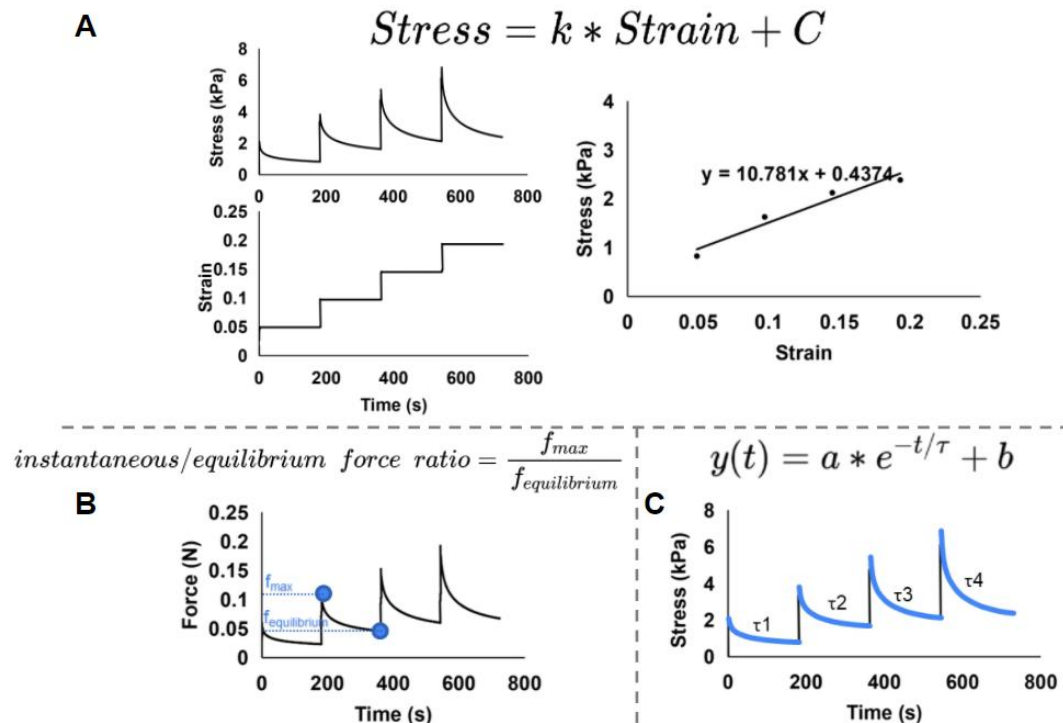


Figure 3 Data process of viscoelastic properties quantification. (A) The equilibrium stress is plotted as a function of strain, and the Young's modulus is estimated as the slope of the linear fit to the stress-strain data. (B) Instantaneous / equilibrium force ratio is the ratio of maximum and equilibrium force in each step, indicating how much stress the tissue released to reach a lower equilibrium point. (C) Relaxation time constant evaluates the time of how long it takes for the tissue stress level to relax and become stable.

RESEARCH AIMS AND DESIGN

Since residual solid stress is closely related to tissue development processes like growth and morphogenesis, which can conversely affect tissue physiology, it is important to investigate the residual solid stress in organs at different stages of development.

Previously, it has been demonstrated that residual solid stress can be quantified in *ex vivo* organs via slicing tissues embedded in agarose and imaging their deformation after tissue relaxation using ultrasound [20]. It was shown that slicing a murine kidney resulted in small deformations after tissue relaxation, thus it has negligible residual solid stress [20]. Previous research also showed that sustained stress exists in murine brain, but there's a lack of information on residual solid stress levels in it. Thus, in this research, I optimized and validated the slicing method for evaluating the residual solid stress level in murine brain and kidney (as a negative control). Mapped the evolution of residual solid stress and viscoelastic changes with age in murine brain, and also studied the residual solid stress distribution in the whole murine brain.

Aim 1: Optimize and validate residual solid stress quantification methodology in the murine organs

Quantify residual solid stress with normalized deformation as an index of residual solid stress

Brain and kidney were dissected from sacrificed mice and kidney was used as a negative control due to its negligible residual solid stress. The freshly dissected tissue was processed with the slicing method to remove the mechanical confinement at the cut surface such that it could deform. The deformation is a measure of the stored energy in

the tissue caused by residual solid stress. The cross-section view of the slices was used to directly show the deformation curve on the slice surface. The extent of deformation was quantified as normalized deformation, the average height difference from the curved surface to the midline, to compared between tissue (Fig.4A), and did statistics analysis to show the significant difference. Two representative slices from kidney and brain showed how the normalized deformation can indicate extent of deformation and the stress level. On kidney slice, the surface points were all close to the midline, and had a lower normalized deformation which showed it had small deformation and low residual solid stress (Fig.4B). On brain slice, the surface points had various distances to the midline, and had a higher normalized deformation, which showed brain slice had a larger deformation and higher stress level (Fig.4C). Such a quantification would be an evaluation of residual solid stress level in tissue slices.

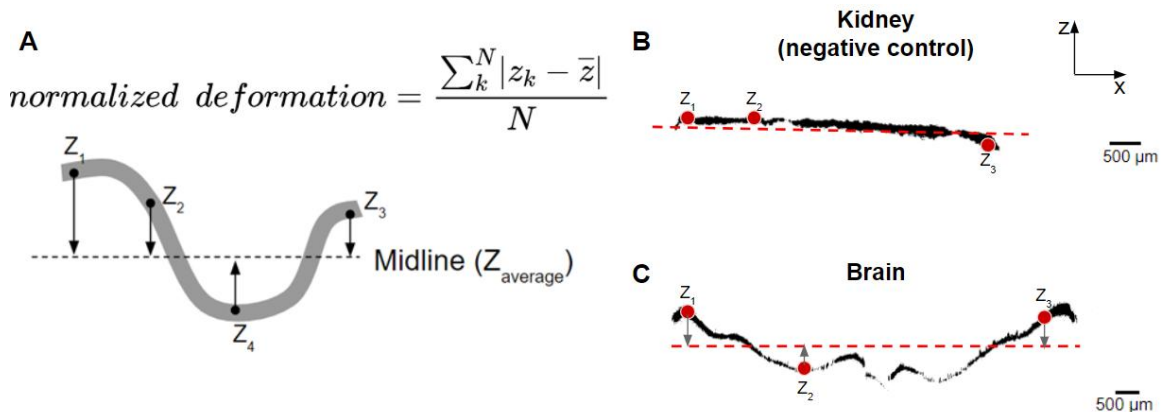


Figure 4 Normalized deformation quantification. (A) The normalized deformation, an index of residual solid stress, is defined as the average height difference from curved surface to the midline. (B) The cross-section view of a representative kidney slice. (C) The cross-section view of a representative brain slice.

Micron-scale of deformation map

Besides quantifying the deformation as normalized deformation, built deformation maps at micron-scale for obvious comparison of deformation extent between brain and kidney, and was able to show the distribution of deformation on the slices.

Ionic strength effect to deformation

In the slicing method, the slices were immersed in PBS for deformation due to stress relaxation after the fresh tissue been sliced. In tissue experiments, PBS is often used to maintain tissue hydration during mechanical testing, the solutes from the buffer can diffuse into the tissue and interact with its structure and mechanics [23]. As the ionic strength is understood to have effect on tissue mechanics [24], it would be meaningful to study the relationship between the ionic strength in PBS, and the deformation on the slices. I set four groups of ionic strength through using different concentration of PBS, including 0.01X, 0.1X, 1X, and 10X PBS. Among the four groups, the 1X PBS was the physiological condition and was used in normal experiment, so it was used as the control group in this experiment. The slices were immersed in specific buffer immediately after slicing for tissue deformation. Then hold the deformed slices in 1% agarose made by corresponding 0.01X, 0.1X, 1X and 10X PBS, fixed with formalin and imaged with confocal microscopy. Finally compared the deformation maps and the normalized deformation quantification.

Validation experiments

Three validation tests were done to support the data reliability of the slicing method.

First, since the tissue slice was immersed in PBS for the deformation occur, I did a flipping test for avoid the possibility that the deformation was an artifact caused by the buoyancy. The buoyancy might have different pressure acting on opposite sides of the slice, and thus the heavy part will sink and the light part will go up and floating in the liquid, and result to deformation. I did the flipping test through imaging the slice immediately after tissue deformed, and then flip the slice to upside down and then image again. These all steps will be finished before the tissue degradation. Then compared the cross-section view and the normalized deformation quantification.

The second validation test was to evaluate the artifact due to fixation. In the slicing method, I used formalin to fix the tissue and avoid tissue degradation. To test if the fixation process could affect the deformation or not, I imaged the brain slice after it deformed and hold in 1% agarose, and then do the fixation with formalin, wash with PBS, after that did another imaging, and compare the cross-section view, deformation maps, and normalized deformation quantification.

The third validation test was to test the normalized deformation accuracy of showing the extent of residual solid stress through slicing the heart. The heart is studied previously as an organ which has a strong residual stress in it [21]. I used the same slicing method to slice the murine heart, compared the deformation maps and normalized deformation quantification between organs, to see if the normalized deformation can

show the extent of residual solid stress.

Aim 2: Map evolution of residual solid stress changes in the murine brain with age

Evolution of residual solid stress in murine brain with age

Investigating the accumulation of residual solid stress as a function of tissue growth provides invaluable information regarding both the genesis and implications of residual solid stress. I used the slicing method to measure the normalized deformation, induced by the relaxation of residual solid stress, among three different age groups, including 5–7 days, 8–12 weeks, and 22 months. After compared the residual solid stress level between brain and kidney in aim 1, I focused on the changing tendency of normalized deformation here, and also fit the changing trend to the human brain volume changing chart from previous research [15] and showed the potential relationship between brain volume and residual solid stress changes.

Evolution of viscoelastic properties in murine brain with age

I analyzed the changes of viscoelastic properties in the normal murine brain with age. The viscoelastic properties of the tissues were measured via Instron with an unconfined compression test for three different age groups of mice, including 5–7 days, 8–12 weeks, and 22 months. I quantified the Young's modulus, instantaneous / equilibrium force ratio, and relaxation time constant, and showed their changing tendency with age.

Residual solid stress distribution in the whole brain

Besides quantifying the residual solid stress in individual brain slices, I sliced the whole brain from 8–12 weeks mice to get 18 continuous slices at the coronal direction with each slice 250 μm thick, and totally 4500 μm in distance. Then I created deformation maps and normalized deformation quantification to study the distribution of residual solid stress in brain at the coronal direction.

RESULTS

Aim 1

Quantify residual solid stress with normalized deformation as an index of residual solid stress

With the cross-section view, tissues with negligible residual solid stress, such as normal kidney [20], the slices had flat surface and the deformation was negligible (Fig. 5A). Brain slices had curved surfaces and larger deformation (Fig. 5A). The normalized deformation for the brain was significantly higher than the control tissue kidney in all 3 age groups (Fig. 5B), which showed that the brain has a larger residual solid stress than the kidney.

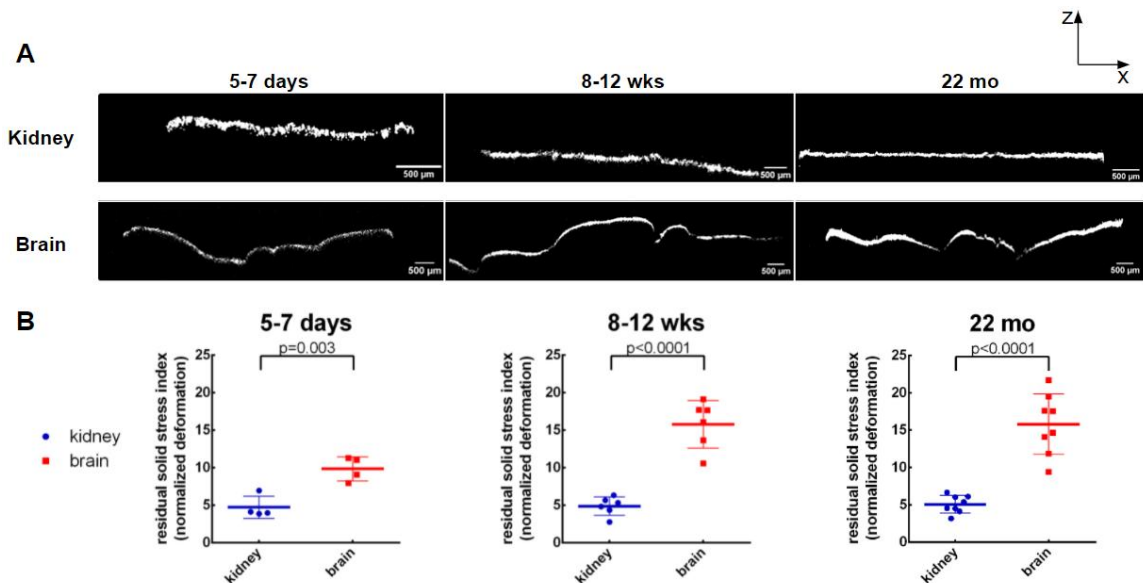


Figure 5 Quantify residual solid stress with normalized deformation as an index of residual solid stress. (A) The orthogonal views of deformation of representative brain and kidney slices from 5–7 days, 8–12 weeks, and 22 months mice. (B) The normalized deformation quantification of brain and kidney slices from 5–7 days, 8–12 weeks, and 22 months mice. The projections and deformation maps of representative slices from the brain and kidney.

Micron-scale of deformation map

The Z projection of the binary confocal image directly show the slice shape and boundary. The deformation maps of kidney slices showed the flat surface among 3 age groups and the deformation were negligible and uniform across the cut surface, thus lower residual solid stress interior. Compared to kidney, the deformation maps of brain slices indicated larger deformation which unevenly distributed across the cut surface and thus higher residual solid stress interior (Fig. 6).

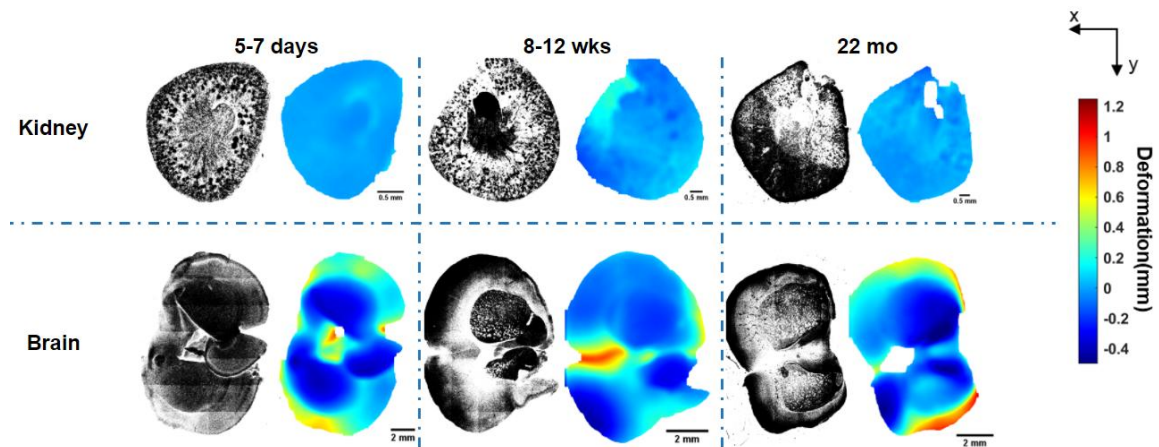


Figure 6 The projections and deformation maps of representative brain and kidney slices from 5–7 days, 8–12 weeks, and 22 months mice.

Ionic strength effect to deformation

From the deformation maps, larger deformation occurred in slices immersed in 0.01X and 0.1X PBS, compared to 1X PBS, which focused on the edges of slices and caused folding, slices immersed in 10X PBS seems didn't have any obvious difference compared to 1X PBS (Fig. 7A). With the normalized deformation quantification, slices immersed in 0.01X and 0.1X PBS both have significantly higher normalized deformation than slices immersed in 1X PBS, and there's no significant difference between 0.01X and

0.1X, which means that lower PBS concentration, the lower ionic strength could cause larger deformation on brain slices. Between slices immersed in 1X and 10X PBS, there's no significant difference in normalized deformation, which means higher PBS concentration, the higher ionic strength, won't affect much on the tissue deformation (Fig.7B).

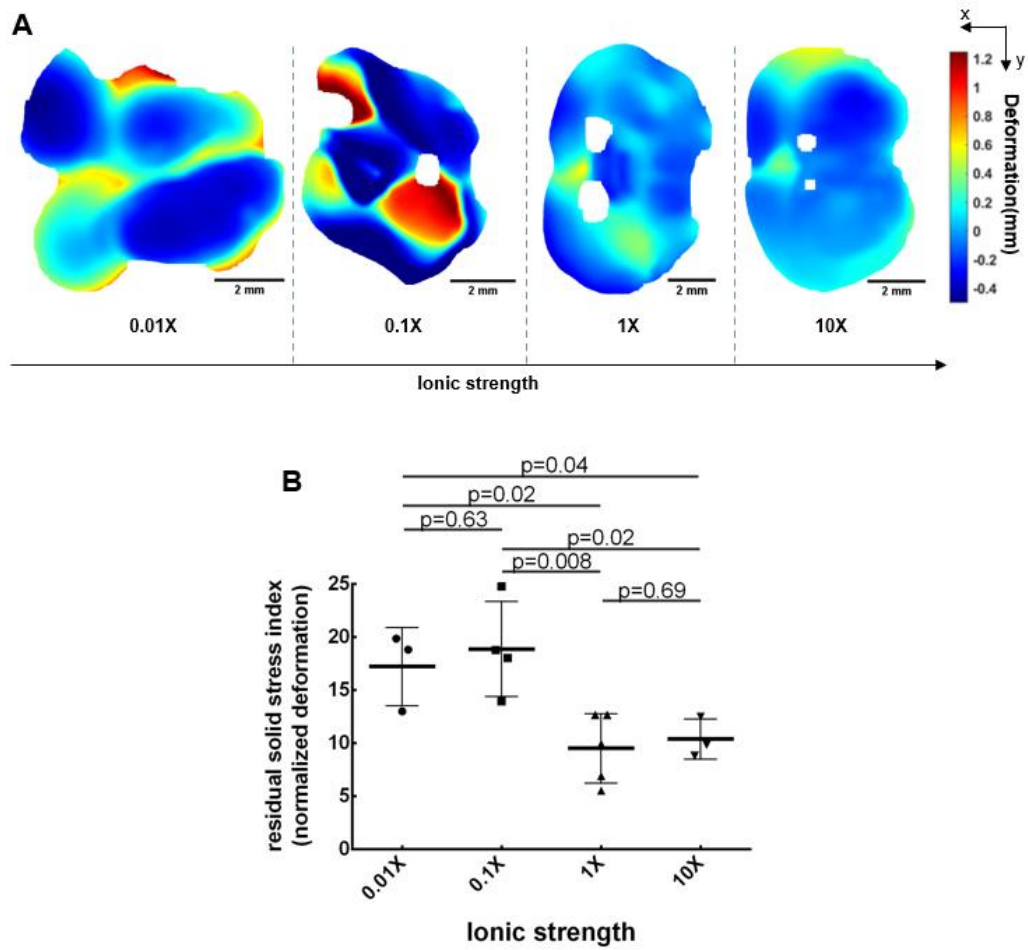


Figure 7 The effect of different ionic strength to tissue deformation. (A) The deformation maps of representative brain slices under different ionic strength. (B) The normalized deformation statistics of brain slices under different ionic strength.

Validation experiments

From the flipping test, the cross-section views of the slice from initial and after flipping stages had symmetrical curve (Fig.8A), and with normalized deformation statistics, there's no significant difference between the normalized deformation value from two stages (Fig.8B). Which showed that the buoyancy had no significant effect on normalized deformation, and thus won't cause artifact on deformation.

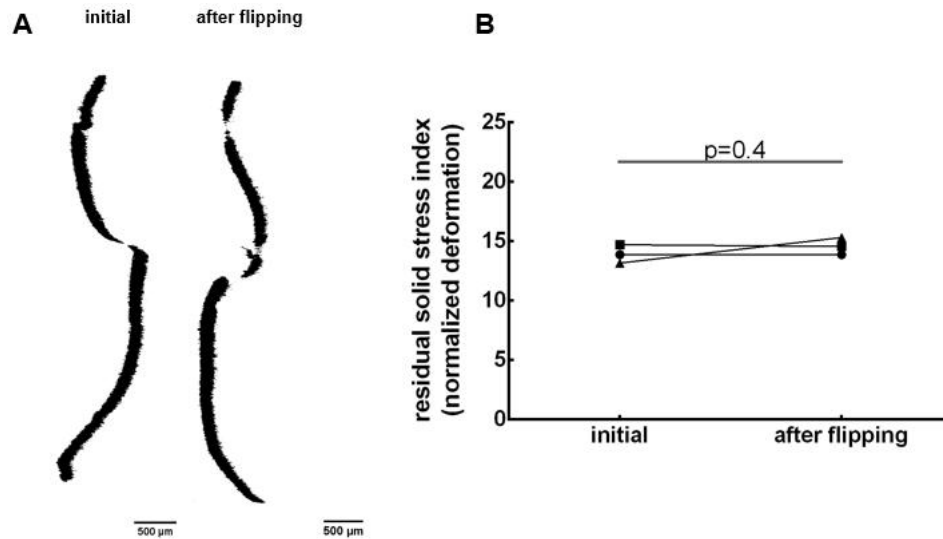


Figure 8 Flipping test to avoid buoyancy artifacts. (A) The orthogonal view of representative slices before and after flipping. (B) Statistics of normalized deformation with no significant difference between initial and after flipping.

From the fixation test, the cross-section views of the slice were similar before and after fixation, and the deformation maps from two images were also similar (Fig. 9A). With the normalized deformation statistics, there had no significant difference between the fresh and fixed slices (Fig.9B). Which showed that fixation won't cause artifact on deformation.

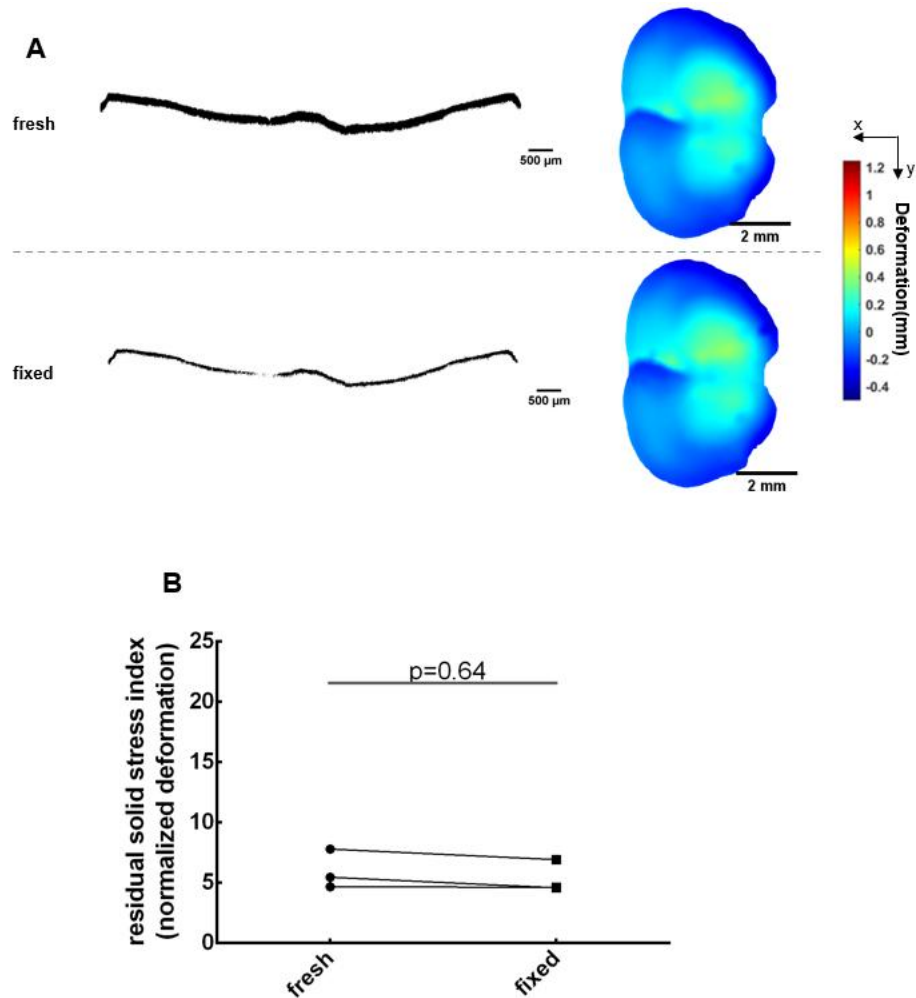


Figure 9 Fixation test for evaluating potential artifacts due to formalin fixation. (A) The orthogonal view and deformation maps of representative brain slices from fresh and fixed states. (B) Statistics of normalized deformation shows that there's no significant difference between fresh slices and fixed slices.

Through slicing the heart with the slicing method, from the deformation map, the heart slice had a larger deformation compared to kidney and was unevenly distributed (Fig. 10A). With the normalized deformation statistics, the heart had a significant higher normalized deformation than kidney (Fig.10B). It showed the higher residual solid stress level in heart, which was corresponding to the previous research that heart was an organ

contained high stress interior, and supported the accuracy of our slicing method in evaluating the residual solid stress level through measuring the deformation.

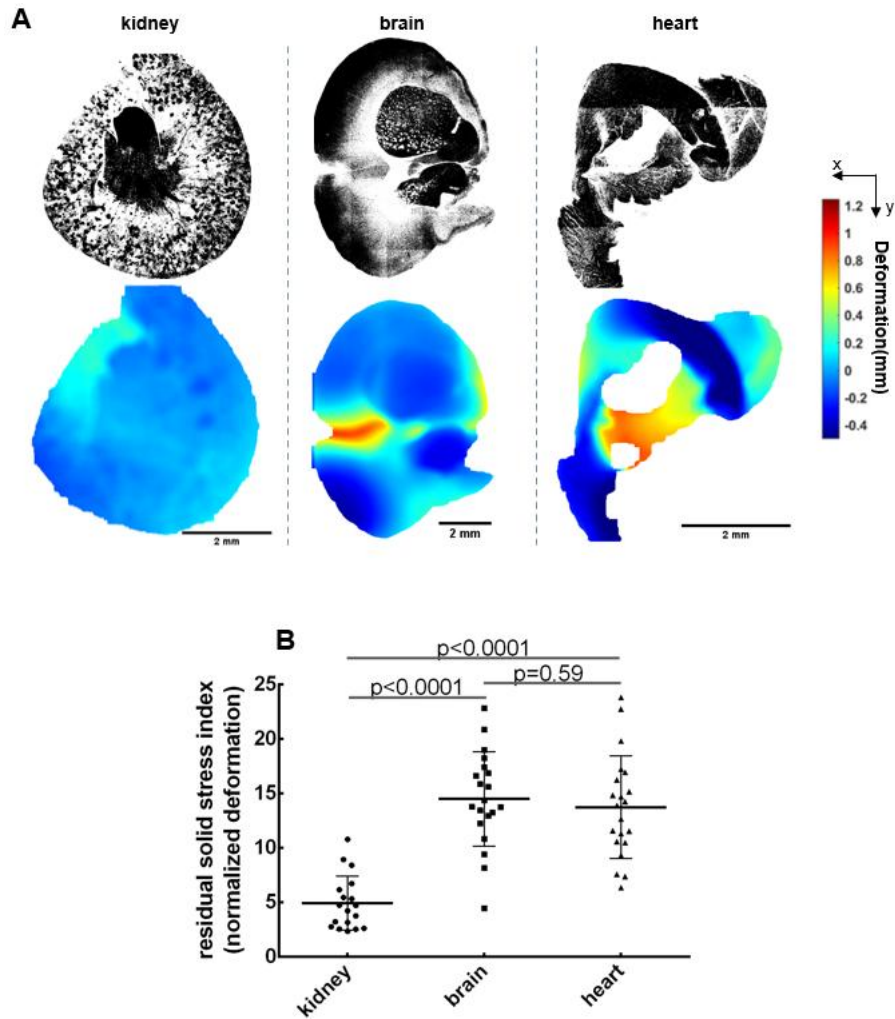


Figure 10 Quantification of residual solid stress in heart. (A) The projections and deformation maps of representative slices from kidney, brain, and heart. (B) Statistics of normalized deformation shows that heart tissue had a higher residual solid stress than kidney tissue.

Aim 2*Evolution of residual solid stress in murine brain with age*

After comparing the residual solid stress between kidney and brain and showed the higher residual solid stress level in murine brain in aim1, here I showed the changing tendency of residual solid stress level in organs with age. Kidney maintained the same low value in all 3 age groups, which showed its low residual solid stress among all development stages as a negative control. The normalized deformation in brain slices increased significantly with the age increase from 5–7 days to 8–12 weeks, and then remained the same from 8–12 weeks to 22 months. Which means the 5–7 days mice had lower residual solid stress in brain, and stress were increasing while the mice growing up, and become stable from its maturation to aging (Fig. 11A). The rapid increase in early development stage indicated that there might be a relationship between residual solid stress and rapid tissue growth in this early development.

I fitted this changing tendency of residual solid stress in brain to the volume changes which is from previous research [13,15,22]. I converted the mice age to human age as showed in previous study [25], that 5–7 days mice equal to 0.1 years human, 8–12 weeks mice equal to 20 years human, 22 months mice equal to 80 years human. There existed both rapid increases of normalized deformation and white matter volume in the early development stage, including the late infancy and late childhood. The tendency of normalized deformation changing reaches the highest value at the similar age range when the white matter volume becomes the largest in brain, which consistently indicated that the residual solid stress in brain could interact with the tissue structure development, such

as size increasing (Fig. 11B).

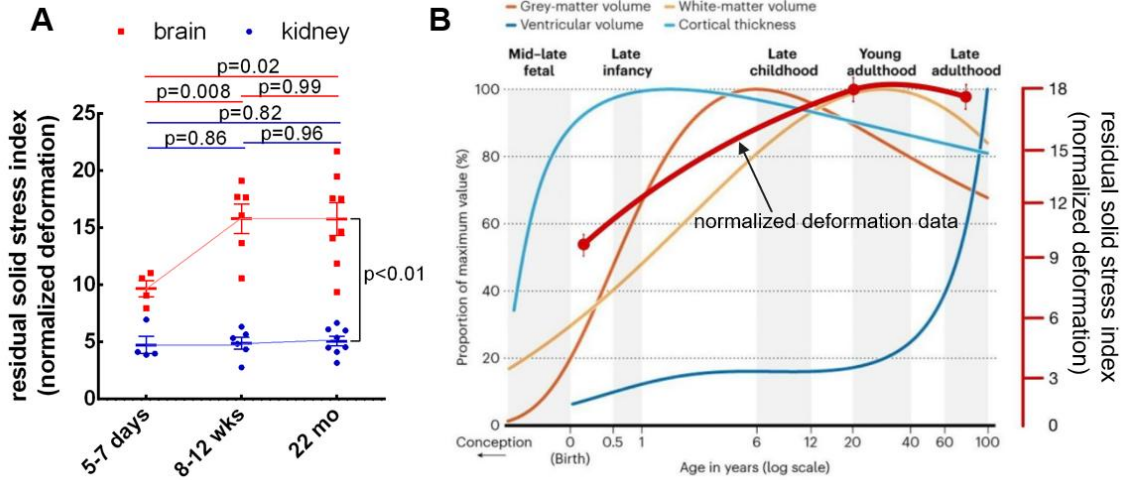


Figure 11 Evolution of residual solid stress in the brain by age. (A) The normalized deformation changing tendency in brain and kidney slices with age. Brain slices have a significant increase in normalized deformation from 5–7 days to 8–12 weeks, and remain the same from 8–12 weeks to 22 months. Kidney maintains the same value of normalized deformation among three age groups. (B) The normalized deformation trend with age in the brain compared to the volume changes. Mice age was converted to equal human age to fit the plot. Normalized deformation and the white-matter volume reach the highest value at similar ages. Modified from [13, 15, 22].

Evolution of viscoelastic properties with age

I analyzed the changes of viscoelastic properties in the normal brain with age.

Young's modulus significantly increased from 5–7 days to 8–12 weeks, and then decreased from 8–12 weeks to 22 months (Fig. 12A), showed the brain was soft in the early stage and reached its most stiff stage at maturation, then became softer than mature but still more stiff than early stage when aging. Instantaneous / equilibrium force ratio had a slight trend to decrease from 5–7 days to 22 months (Fig. 12B), showed that the brain released more internal stress during the early stage. The relaxation time constant, decreased significantly from 5–7 days to 8–12 weeks, and remained lower at 22 months (Fig. 12C), showed that the brain from the early development stage needs more time to

release the stress and reach equilibrium.

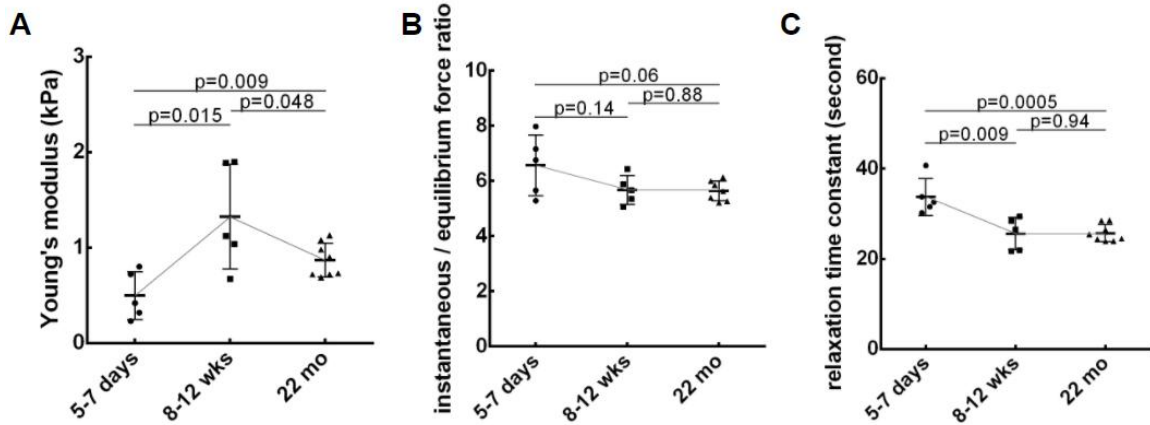


Figure.12 Evolution of viscoelastic properties in the brain by age. (A) Young's modulus in the brain increases from 5–7 days to 8–12 weeks, then decreases to 22 months. (B) The instantaneous / equilibrium force ratio in the brain has no significant difference among three age groups, but has a decreasing tendency from 5–7 days to 22 months. (C) The relaxation time constant in the brain decreases from 5–7 days to 8–12 weeks, then keeps plateau to 22 months.

Residual solid stress distribution in whole brain

With the increased distance, the first couple slices from 0–1000 μm distance, had lower normalized deformation and flat surface with smaller deformation, low residual solid stress, and also smaller sizes. The following couple slices from 1000–2250 μm , experienced a rapidly increase of normalized deformation with increasing deformation, residual solid stress, and also increasing size. The relatively-plateaued normalized deformation at the distance about 2500–3750 μm showed the stable residual solid stress at this location, and also with similar deformation maps. The normalized deformation then had another increase at the distance of 3750–4500 micron, which indicated the higher deformation and residual solid stress at this point. The overall tendency showed that normalized deformation and deformation maps increase along the coronal brain slices, which was the distance (Fig.13). It indicated that the front part of brain contained

lower residual solid stress, higher residual solid stress existed in the middle and back part of the brain.

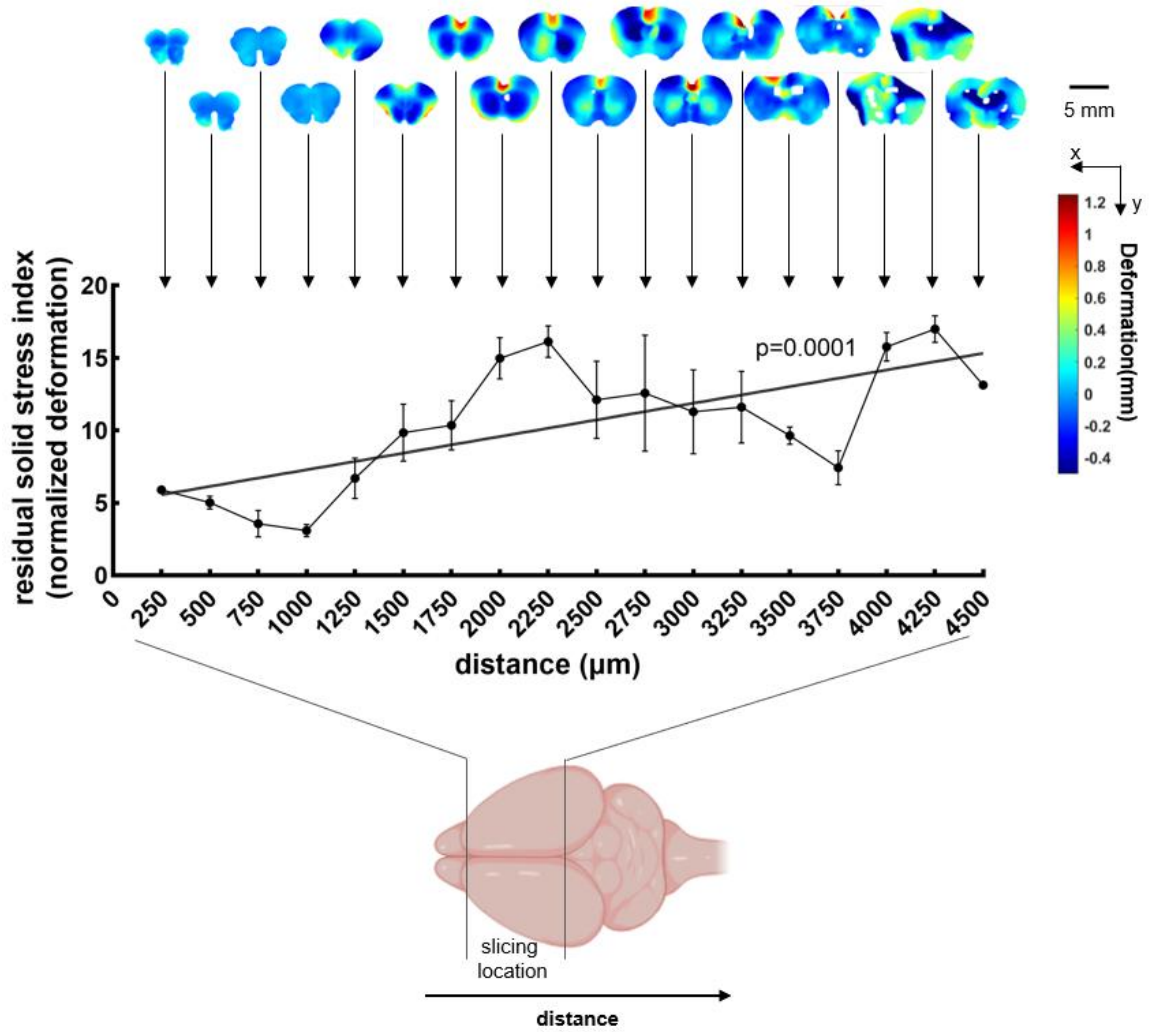


Figure 13 The normalized deformation and deformation maps from the brain at a coronal direction. The residual solid stress level had an overall increasing trend with the distance.

DISCUSSION

Based on the fundamental concept that tissues containing residual solid stress undergo deformation after release of physical confinement, we utilized the slicing method to quantify the deformation and the extent of residual solid stress in murine brains. Investigating the accumulation of residual solid stress as a function of tissue growth provides invaluable information regarding both the genesis and implications of residual solid stress. Our slicing method, based on releasing residual solid stress by creating thin tissue slices, provides a sensitive method to quantify low levels of residual solid stress in small specimens. The tissue slice, originally flat, undergoes bending in the area of the slice where the residual solid stress is released [20]. This method is sensitive as a thin slice can react to small values of residual solid stress due to the small thickness of the slice (Fig.1). Viscoelastic properties are important in biological tissues as constituents of tissues such as cells, extracellular matrices, and structural proteins, are viscoelastic [26]. We also studied the viscoelastic properties through an unconfined compression test, including Young's modulus, instantaneous / equilibrium force ratio, and relaxation time constant (Fig. 3, 12).

This study informs understanding of the tissue development process at multiple levels. We presented the higher residual solid stress in the murine brain compared to the kidney with visualization as a deformation map and quantification as a normalized deformation (Fig. 5, 6). The brain has changes in residual solid stress during different ages (Fig. 11) as an increased residual solid stress level from early stage to mature and plateau until aging. The correlation of normalized deformation and brain white matter

volume changing tendency (Fig. 11) suggest that the structural changes in tissue growth are influenced by the stress inside the tissue. With the distribution of residual solid stress inside the whole brain (Fig. 13), it can help study the brain mechanics with its structure, such as cell and molecular contribution, and its function.

This research shows the residual stress remains stable in the mature murine brain. Further studies on mice with older ages, or with brain atrophy caused by aging would be interesting to pursue. Additionally, this research provides a method to compare the extent of residual solid stress in the brain through quantifying the deformation, but has a lack of quantification of the specific residual solid stress, which can be improved in the future with combined analysis of tissue modulus.

CONCLUSION

In this study, we used the slicing method to evaluate residual solid stress in tissue slices by quantifying the deformation with normalized deformation. We studied the evolution of residual solid stress changes in the murine brain with age, and found the significant increase in the early stage of tissue growth and development. We also investigated the viscoelastic properties changes in the murine brain, which can help analysis of residual solid stress evolution. We mapped the distribution of residual solid stress in the whole brain, and showed the stress increased along coronal brain slices. The method and results shown here support further study of the relationship between tissue growth and the residual solid stress in the developing murine brain.

BIBLIOGRAPHY

1. Nia, H.T., L.L. Munn, and R.K. Jain, Physical traits of cancer. *Science*, 2020. 370(6516).
2. Fletcher, D.A. and R.D. Mullins, Cell mechanics and the cytoskeleton. *Nature*, 2010. 463(7280): 485–492.
3. Kalli, M. and T. Stylianopoulos, Defining the Role of Solid Stress and Matrix Stiffness in Cancer Cell Proliferation and Metastasis. *Frontiers in Oncology*, 2018. 8: article 55.
4. Rosen, J., et al., Biomechanical properties of abdominal organs in vivo and postmortem under compression loads. *Journal of Biomechanical Engineering*, 2008. 130(2): 021020.
5. Marasco, G., et al., Role of liver and spleen stiffness in predicting the recurrence of hepatocellular carcinoma after resection. *Journal of Hepatology*, 2019. 70(3): 440–448.
6. Seano, G., et al., Solid stress in brain tumours causes neuronal loss and neurological dysfunction and can be reversed by lithium. *Nature Biomedical Engineering*, 2019. 3(3): 230–245.
7. Amidei, C. and D.S. Kushner, Clinical implications of motor deficits related to brain tumors(dagger). *Neuro-oncology Practice*, 2015. 2(4): 179–184.
8. Helmlinger, G., et al., Solid stress inhibits the growth of multicellular tumor spheroids. *Nature Biotechnology*, 1997. 15(8): 778–783.
9. Fung, Y.C. and S.Q. Liu, Change of residual strains in arteries due to hypertrophy caused by aortic constriction. *Circulation Research*, 1989. 65(5): p. 1340–1349.
10. Burton, K. and D.L. Taylor, Traction forces of cytokinesis measured with optically modified elastic substrata. *Nature*, 1997. 385(6615): 450–454.
11. Tau, G.Z. and B.S. Peterson, Normal development of brain circuits. *Neuropsychopharmacology*, 2010. 35(1): 147–168.
12. Grydeland, H., et al., Waves of Maturation and Senescence in Micro-structural MRI Markers of Human Cortical Myelination over the Lifespan. *Cerebral Cortex*, 2019. 29(3): 1369–1381.
13. Kozlov, M., Your brain expands and shrinks over time – these charts show how. *Nature*, 2022. 604(7905): 230–231.

14. Chen, Z., et al., How the embryonic chick brain twists. *Journal of the Royal Society. Interface*, 2016. 13(124).
15. Bethlehem, R.A.I., et al., Brain charts for the human lifespan. *Nature*, 2022. 604(7906): 525–533.
16. Oatridge, A., et al., Change in brain size during and after pregnancy: study in healthy women and women with preeclampsia. *AJNR. American Journal of Neuroradiology*, 2002. 23(1): 19–26.
17. Hoekzema, E., et al., Pregnancy leads to long-lasting changes in human brain structure. *Nature Neuroscience*, 2017. 20(2): 287–296.
18. Xu, G., P.V. Bayly, and L.A. Taber, Residual stress in the adult mouse brain. *Biomechanics and Modeling in Mechanobiology*, 2009. 8(4): 253–262.
19. Nia, H.T., et al., In vivo compression and imaging in mouse brain to measure the effects of solid stress. *Nature Protocols*, 2020. 15(8): 2321–2340.
20. Nia, H.T., et al., Solid stress and elastic energy as measures of tumour mechanopathology. *Nature Biomedical Engineering*, 2016. 1: 0004. <https://doi.org/10.1038/s41551-016-0004>
21. Taber, L.A., Biomechanics of cardiovascular development. *Annual Review of Biomedical Engineering*, 2001. 3: 1–25.
22. Marek, S., et al., Reproducible brain-wide association studies require thousands of individuals. *Nature*, 2022. 603(7902): 654–660.
23. Safa, B.N., et al., Exposure to buffer solution alters tendon hydration and mechanics. *Journal of Biomechanics*, 2017. 61: 18–25.
24. Nguyen, A.M. and M.E. Levenston, Comparison of osmotic swelling influences on meniscal fibrocartilage and articular cartilage tissue mechanics in compression and shear. *Journal of Orthopaedic Research*, 2012. 30(1): 95–102.
25. Dutta S and Sengupta P, Men and mice: Relating their ages. *Life Sciences*, 2016. 152: 244–248.
26. Chaudhuri O., et al., Effects of extracellular matrix viscoelasticity on cellular behaviour, *Nature*. 2020. 584(7822): 535–546.

CURRICULUM VITAE

